Journal of Dental Research
2019, Vol. 98(6) 659–665

DOI: 10.1177/0022034519837245
journals.sagepub.com/home/jdr

Disruption of *FOXF2* as a Likely Cause of Absent Uvula in an Egyptian Family

R. Seselgyte[1], D. Bryant[1], C. Demetriou[1], M. Ishida[1], E. Peskett[1], N. Moreno[2], D. Morrogh[3], D. Sell[4], M. Lees[4,5], M. Farrall[6], G.E. Moore[1], B. Sommerlad[4], E. Pauws[2], and P. Stanier[1]

Abstract

This study investigated the genetic basis of an unusual autosomal dominant phenotype characterized by familial absent uvula, with a short posterior border of the soft palate, abnormal tonsillar pillars, and velopharyngeal insufficiency. Cytogenetic analysis and single-nucleotide polymorphism–based linkage analysis were investigated in a 4-generation family with 8 affected individuals. Whole exome sequencing data were overlaid, and segregation analysis identified a single missense variant, p.Q433P in the FOXF2 transcription factor, that fully segregated with the phenotype. This was found to be in linkage disequilibrium with a small 6p25.3 tandem duplication affecting *FOXC1* and *GMDS*. Notably, the copy number imbalances of this region are commonly associated with pathologies that are not present in this family. Bioinformatic predictions with luciferase reporter studies of the FOXF2 missense variant indicated a negative impact, affecting both protein stability and transcriptional activation. *Foxf2* is expressed in the posterior mouse palate, and knockout animals develop an overt cleft palate. Since mice naturally lack the structural equivalent of the uvula, we demonstrated *FOXF2* expression in the developing human uvula. Decipher also records 2 individuals with hypoplastic or bifid uvulae with copy number variants affecting *FOXF2*. Nevertheless, given cosegregation with the 6p25.3 duplications, we cannot rule out a combined effect of these gains and the missense variant on FOXF2 function, which may account for the rare palate phenotype observed.

Keywords: cleft palate, craniofacial biology/genetics, gene expression, oral pathology, speech pathology, transcription factor(s)

Introduction

Clefts of the lip and/or the palate occur in around 1 in 700 births (Mossey et al. 2009). There is a wide phenotypic spectrum that may involve complete or incomplete bilateral or unilateral cleft lip, with or without cleft palate, as well as isolated cleft of the secondary palate. Isolated palate defects are etiologically distinct from cleft lip due to the contribution of different tissue lineages and distinct timing of various fusion events during development (Stanier and Moore 2004; Harville et al. 2005; Mossey et al. 2009). Defects of the secondary palate range from complete cleft of the hard and soft palate or affect the soft palate only. They also include submucous cleft palate (SMCP), where the palatal shelves have fused and the oral mucosa is intact, while a bony notch in the posterior hard palate, translucency in the soft palate (reflecting abnormally inserted levator palati muscles), and a bifid uvula are characteristic features (Calnan 1954; Pauws et al. 2009). When muscle malposition occurs in the absence of the triad of overt signs, it is called occult SMCP (Kaplan 1975). A spectrum of abnormality as well as the functional impact varies between classical and occult SMCP (Sommerlad et al. 2004). Consequences can be mild, remaining undiagnosed (Meskin et al. 1964) or identified incidentally (e.g., during adenoidectomy). In other cases, similar problems to an overt cleft are experienced (Swanson et al. 2017), including significant feeding difficulties with nasal regurgitation, conductive hearing loss due to otitis media, and poor speech (de Blacam et al. 2018). For patients with SMCP, speech may be characterized by hypernasality, audible nasal emission, and the cleft characteristics of passive and nonoral articulation errors, which significantly compromise

[1]Genetics and Genomic Medicine, UCL GOS Institute of Child Health, London, UK
[2]Developmental Biology and Cancer, UCL GOS Institute of Child Health, London, UK
[3]NE Thames Regional Genetics Service Laboratory, Great Ormond Street Hospital NHS Trust, London, UK
[4]North Thames Cleft Centre, St Andrew's Centre, Broomfield Hospital, Chelmsford, UK; Great Ormond Street Hospital for Children NHS Foundation Trust, London, UK
[5]Department of Clinical Genetics, Great Ormond Street Hospital NHS Trust, London, UK
[6]Wellcome Trust Centre for Human Genetics, University of Oxford, Oxford, UK

A supplemental appendix to this article is available online.

Corresponding Author:
P. Stanier, Genetics and Genomic Medicine, UCL GOS Institute of Child Health, 30 Guilford Street, London, WC1N 1EH, UK.
Email: p.stanier@ucl.ac.uk

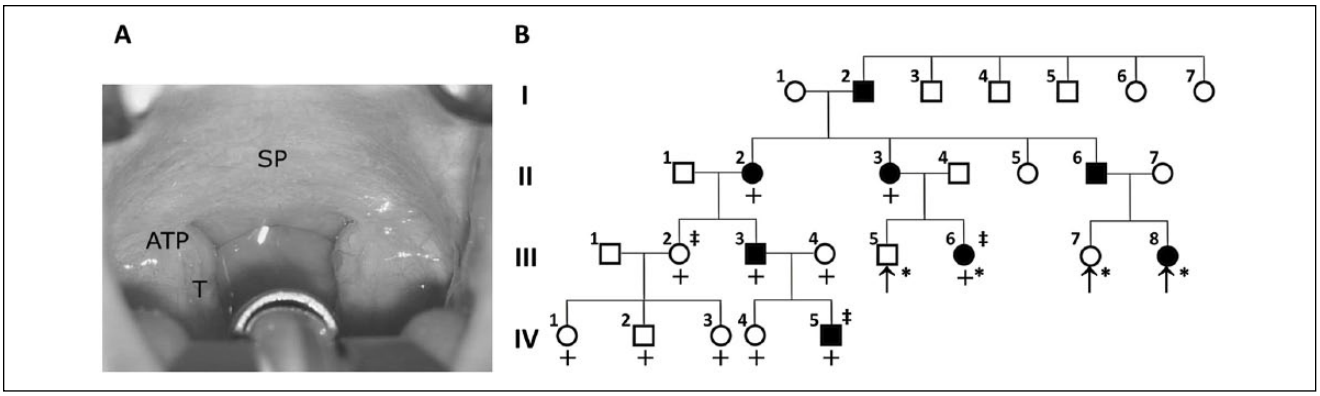

Figure 1. Egyptian family with absent uvula. (**A**) Absent uvula palate in the proband (IV.5). Note the short posterior border of the soft palate where the uvula should be and the unusual structure of the pillar of fauces. ATP, anterior tonsillar pillar; SP, soft palate; T, tonsil. (**B**) Family pedigree showing autosomal dominant inheritance of hypernasality and absent uvula. Eleven family members were genotyped for linkage analysis (+). Exome sequencing analysis was performed on 3 individuals (‡), and Sanger sequencing (*) was used to assess segregation of candidate gene variants in additional individuals (↑).

intelligibility (Sell et al. 1999). This results from effects on the anatomy of the velopharynx. The velopharyngeal mechanism consists of a muscular valve that extends from the posterior surface of the hard palate to the posterior pharynx and includes the soft palate and lateral and posterior pharyngeal walls. The velopharyngeal mechanism creates a tight seal between the velum and pharyngeal walls to separate the oral and nasal cavities during speech and swallowing (Perry 2011; Mardini et al. 2016). Failure of the velopharyngeal sphincter to close may be an anatomic or a physiologic limitation depending on the severity of the palate defect, leading to velopharyngeal insufficiency (VPI).

In this study, we have investigated a highly unusual familial palate defect associated with the clinical presentation of VPI. Affected individuals in an autosomal dominant family present with no uvula, a short posterior border of the soft palate, and an apparent absence of the anterior tonsillar pillars with rudimentary posterior pillars (Fig. 1). To investigate the genetic basis of this condition, we report our genetic studies, which identify small 6p25.3 duplications cosegregating with a missense variant in FOXF2 as the likely cause of this condition.

Materials and Methods

Patients and Clinical Evaluation

The pedigree consists of a 4-generation Egyptian family with autosomal dominant hypernasality and absent uvula with a short posterior border of the soft palate and abnormal tonsillar pillars (Fig. 1). Specialist speech pathology assessment was undertaken for IV.5. Perceptual examination revealed mild hypernasality with cleft speech characteristics (Sell et al. 1999). A diagnosis of VPI was based on lateral videofluoroscopy, which showed a thin velum with poor lift. Also, there were small adenoids above and at the plane of attempted closure, with some slight movement of the posterior pharyngeal wall. The medical history included feeding difficulties with nasal regurgitation after birth. No other medical issues were recorded. Visual inspection and digital recording of oral pathology for IV.5 and other family members were also conducted.

Detailed materials and methods are included in the Appendix.

Results

An Egyptian boy (IV.5) presented with a clinical history of occasional nasal regurgitation while breastfeeding in infancy, followed by speech and language delay and hypernasality. On examination at 3 years, the patient's uvula was absent, and the posterior border of the soft palate appeared short; the anterior tonsillar pillar was also absent, while the posterior pillar was rudimentary (Fig. 1A). There was poor velar movement. There were no obvious syndromic features. The family history revealed 7 other individuals with no uvula and a tight posterior border of the velum and pillar structure (Fig. 1B). All affected family members had mild hypernasal speech.

Genome-wide cytogenomic microarray analysis of the proband excluded a deletion at 22q11.2 but indicated the presence of 2 duplications on 6p25.3 (Appendix Fig. 1). A small gain (227,481 bp) overlapped only with a single predicted but uncharacterized noncoding mRNA (LOC285768) and a 480,000-bp gain encompassing *FOXC1* and the 5′ exons of *GMDS*. A quantitative polymerase chain reaction assay for *FOXC1* confirmed the presence of the copy number variation (CNV) and demonstrated inheritance from the father and his paternal grandmother, who both had palates of similar appearance and mild hypernasality. The variant was not present in the proband's mother.

Linkage Analysis

Single-nucleotide polymorphism (SNP)–based genotyping was performed on 11 individuals from the family (Fig. 1B). III.5, III.7, and III.8 were unavailable at this time. Quality

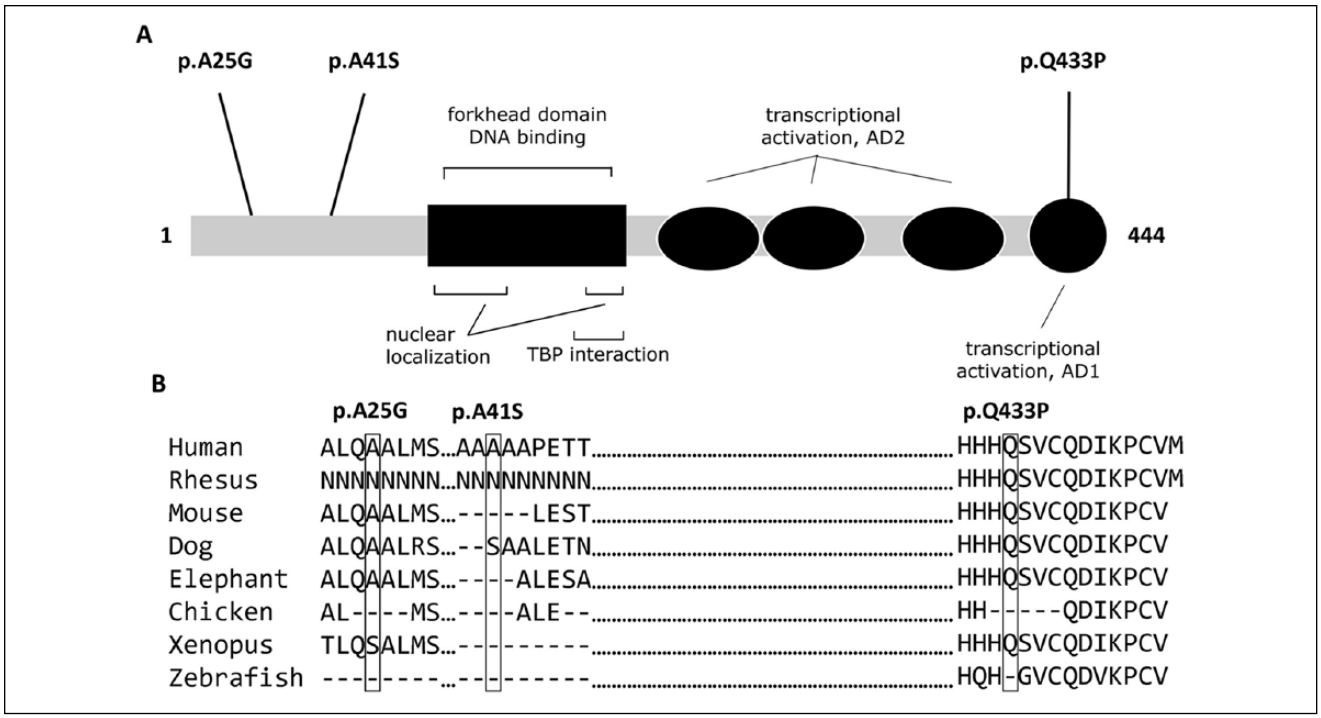

Figure 2. The functional domains of *FOXF2*. (**A**) The locations of nonsynonymous missense variants p.A25G, p.A41S, and p.Q433P are given. Note that the 2 N-terminal variants p.A25G and p.A41S were classified bioinformatically as benign. (**B**) The evolutionary conservation of each variant is indicated in the boxed area.

control analysis indicated no inconsistencies between the "inferred from X-chromosome genotype data" and the recorded sex. The overall genotype missingness rate was very low (>0.003157; a high rate of missing genotype calls can imply poor-quality genotyping). The genome average identity by decent data was consistent with the communicated family structure. Following quality control, a set of 5,497 informative autosomal SNPs located at approximately 0.5-cM spacing were selected for parametric linkage analysis. These SNPs captured 89% (SE, 4.2%) of the theoretical maximal linkage information in the family. Ten regions fully segregated with the phenotype, reaching the maximum LOD score of 1.5 (logarithm of the odds). One small region narrowly failed to reach this score (Appendix Fig. 2). Collectively, these intervals contained approximately 760 RefSeq genes and spanned a little over 100 million bases. The likely causal gene was expected to segregate with one of these intervals.

Exome Sequencing

Exome sequencing was performed on 2 affected individuals (IV.5 and III.6) and 1 unaffected female (III.2) who had 3 unaffected children (Fig. 1B). Sequencing data were analyzed as described in the Appendix. Twenty-one candidate variants were present in both affected individuals but not in the unaffected individual. Eleven of these were excluded following alignment to the linkage data. The 10 remaining variants were therefore considered candidates. Each variant was validated with Sanger sequencing. Details of each candidate variant (*PLB1, FOXF2, SNX10, PLIN2, IGDCC3, THSD4, SEMA7A, SCAPER, SH2D7*, and *IL16*) are presented in Appendix Table 1 and bioinformatics analysis in Appendix Table 2. Three additional family members (III.5, III.7, III.8; Fig. 1B) were later recruited, and Sanger sequencing was conducted to investigate segregation for each of the 10 variants. Only the c.1298A>C (p.Q433P) variant in *FOXF2* fully segregated with the phenotype and was therefore considered the most likely pathogenic variant (Appendix Fig. 3). By incorporating the new individual's variant genotypes from each candidate locus as additional SNPs into the linkage analysis, the LOD score at 6p25.3 increased to 1.9. At each of the other loci, LOD scores reduced to between −0.4 and 1.4.

The *FOXF2* c.1298A>C variant was reported twice in 2 heterozygous European individuals of unknown phenotype in the gnomAD and ExAC databases. No other information was reported about these individuals. Two further missense substitutions were also reported at the same position, p.Q433H (Latino) and p.Q433G (East Asian), at 1 of 246,272 alleles. In terms of amino acid conservation, the glutamine residue is well conserved across species, excluding chicken and lamprey (Fig. 2). Interestingly, the *FOXF2* variant is very close to and in linkage disequilibrium with the 6p25.3 tandem duplication identified by the cytogenetic analysis.

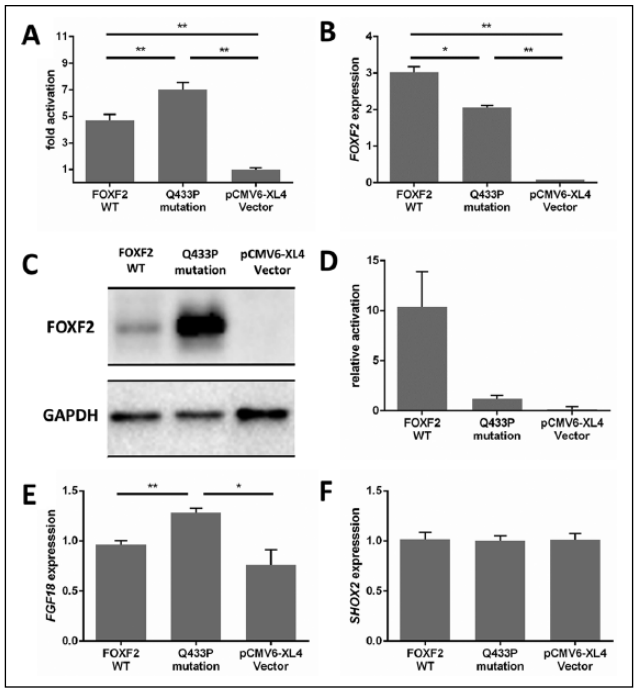

Figure 3. Functional analysis of the FOXF2 p.Q433P variant. (**A**) Transcriptional activation of FOXF2 WT and Q433P constructs in HeLa cells. Data represent the mean ± SD of triplicate samples at 24 h posttransfection. (**B**) Quantitative expression difference between the WT and p.Q433P mutation constructs measured by RTqPCR in HeLa cells. (**C**) Western blot shows FOXF2 protein expression in HeLa cells transfected with FOXF2 WT, Q433P mutation, and pCMV6-XL "empty" vector constructs. (**D**) Transcriptional activity normalized to protein level. (**E**) *FGF18* and (**F**) *SHOX2* transcript levels assessed by RTqPCR and normalized to *ACTB* in HeLa cells at 24 h following transfection of WT, Q433P constructs, and empty vector. All data presented are representative of at least 3 replicate experiments. *$P < 0.05$. **$P < 0.01$. RTqPCR, quantitative reverse transcription polymerase chain reaction; WT, wild type.

Analysis of FOXF2 *in Individuals with Nonsyndromic Cleft Palate and SMCP*

To investigate whether *FOXF2* pathogenic variants might underlie more common forms of cleft palate, a cohort of patients with nonsyndromic cleft palate ($n = 240$) or SMCP ($n = 72$) was sequenced. Variants identified are listed in Appendix Table 3 and depicted in Figure 2 and Appendix Figure 4. Only 2 rare/unique missense variants were identified (Appendix Fig. 4A, B); neither predicted damaging by bioinformatics analysis (Appendix Table 3). Two common missense variants were also identified (Appendix Fig. 4C, D): at 6:1390576, c.394G>A (p.A132T) was in 170 of 19,842 alleles in Asian heterozygotes in the gnomAD database, while at 6:1390882, c.700C>A (p.P234T) was present in the African population in 182 heterozygotes and 3 homozygotes in 16,934 alleles and 28 of 30,890 Latino heterozygotes. Since these variants were described as benign (Appendix Table 3), they were not studied further. No variants of interest were identified in the coding sequence of *FOXF2* in exome sequencing data generated from ~30 multiplex families with nonsyndromic cleft lip with or without cleft palate from previous genetic studies.

Effect on Transcriptional Activation

Since the p.Q433P variant is located in the previously described activation domain (AD1; Hellqvist et al. 1998; Fig. 2), we investigated the effect of the point mutation on FOXF2 transcriptional activity with transient luciferase reporter assays. Wild type (WT) and p.Q433P constructs were cotransfected into HeLa cells with a FOXF2 luciferase reporter plasmid, which contained 4 consecutive FOXF2 binding sites (Hellqvist et al. 1998). WT and p.Q433P constructs both produced significant activation as compared with empty vector, while the pathogenic variant caused a significant 1.5-fold increase in activation as compared with the WT sequence (Fig. 3A). Interestingly, while a 0.3-fold reduction in quantitative expression difference was observed between the WT and p.Q433P constructs (Fig. 3B), a dramatic and reproducible 11-fold increase in the quantity of the FOXF2-Q433P protein as compared with WT was detected by Western blotting (Fig. 3C). Both constructs were sequenced in their entirety, and plasmid DNA was accurately measured with several methods to ensure even loading. A similar result was reproducibly obtained following transfection into HepG2 cells, and several independent clones gave similar results (data not shown). We also calculated luciferase activity normalized to protein levels (Fig. 3D), since it is not known how the mutation might affect the translation of endogenous FOXF2 protein levels in vivo during embryonic development. This analysis shows effectively an 88% loss of activation relative to the amount of FOXF2 protein present.

Given the findings of Xu et al. (2016), who reported upregulation of *Fgf18* and downregulation of *Shox2* expression in *Foxf2* knockout mice, we investigated the effect of overexpressing *FOXF2* on both these genes in HeLa cells (Xu et al. 2016). Although no effect was detected for *SHOX2, FGF18* was found to be significantly upregulated when overexpressing the FOXF2-Q433P variant in comparison with the WT sequence (Fig. 3E, F; Appendix Fig. 5).

Expression of FOXF2 *in Craniofacial Tissues*

Foxf2 was previously established as being required for normal palate closure in the mouse (Wang et al. 2003), and its expression in the developing orofacial region is restricted to the posterior palate and tongue (Nik et al. 2016; Xu et al. 2016). However, since mice lack a structure equivalent to the uvula, we investigated *FOXF2* expression in coronal sections of human embryos around the time of palatogenesis, using in situ hybridization (Fig. 4). Similar to the mouse, *FOXF2* is expressed in the human embryonic mesenchyme of the oral cavity and tongue. This is particularly notable in the posterior palatal shelves before fusion at Carnegie stages 22 to 23, decreasing significantly in the fused palate found late in the eighth postconception week (L8pcw). Expression was still seen in the most posterior region of the L8pcw embryo, where the palatal shelves had not yet fused and extended to the oral epithelia in addition to the mesenchyme. This region is equivalent to the presumptive uvula.

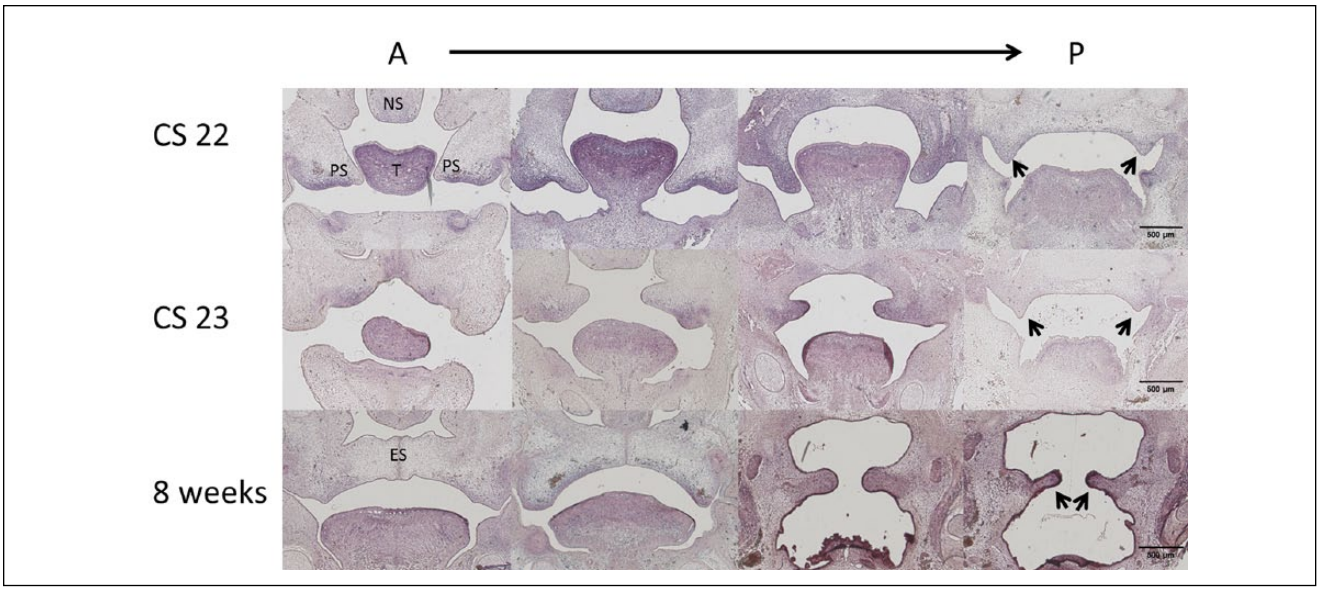

Figure 4. Expression of *FOXF2* in the oral cavity of human embryos. Coronal sections anterior to posterior (left to right) of human embryo heads at CS22, CS23, and L8pcw (top, middle, and bottom panels, respectively), showing maxilla, tongue, and palatal shelves. The second column is approximately midpalate; the third column is toward the back of the palatal shelves; and the fourth column is from among the last sections in each embryo, which show the rudimentary palatal shelves (arrowheads) that will become the uvula upon fusion. Expression of *FOXF2* is seen in the tongue and in the palatal shelves. In the developing palate, expression is mostly on the oral half of anterior regions but becomes more widely expressed throughout the posterior palatal shelf mesenchyme and bordering oral tissues. At later stages, expression includes the more posterior oral epithelial surfaces. ES, epithelial seam; NS, nasal septum; PS, palatal shelf; T, tongue.

Discussion

In this study, we have identified a putative dominantly acting missense mutation in the activation domain of FOXF2, which fully segregates in a multigeneration family that includes 8 affected individuals. All present with absent uvula, short anterior border of the soft palate, and abnormal pillars of the fauces, a rare disorder of palate development. In the mouse, *Foxf2* is expressed in the posterior region of the secondary palate, and homozygous loss of function results in a complete cleft of the secondary palate (Wang et al. 2003). Although mice naturally lack an uvula, we show here that *FOXF2* is also expressed in the posterior human palate during development, including the rudimentary uvula.

The *FOXF2* variant was identified with a combination of linkage analysis and exome sequencing, followed by further segregation analysis. Cytogenetic analyses performed during the preliminary investigation revealed 2 small duplicated regions in 6p25.3, which flank *FOXF2* and segregate with the phenotype. The larger of these overlaps with 2 known genes *FOXC1* and *GMDS*. Based on this CNV as a potential cause for the absent uvula phenotype, CNVs of this interval as well as dominant mutations in *FOXC1* are reported to cause glaucoma and/or Axenfeld-Rieger syndrome, which is characterized by Dandy Walker malformation and cerebellar hypoplasia (Gould et al. 1997; Aldinger et al. 2009), sometimes including micro- or hypodontia. Duplications of this interval were also reported, notably in a large pedigree characterized by glaucoma and iris hypoplasia (Lehmann et al. 2000). However, in the Egyptian family, none of the individuals with the duplication display any obvious eye or brain malformation, suggesting that in this respect, the CNV is likely benign. Notably, the *FOXF2* variant lies only ~200 kb distant to the proximal duplication. Decipher lists 52 individuals who have chromosomal gains or losses encompassing this region (Firth et al. 2009). While the majority of these have eye anomalies, 1 individual with a 1.7-Mb duplication including *FOXF2* was reported to have a bifid uvula as well as hyperparathyroidism (Appendix Fig. 1). This CNV was inherited from an unaffected father. Another individual with a small heterozygous deletion including only the *FOXQ1* and *FOXF2* loci (Appendix Fig. 1) was reported to have a hypoplastic uvula and dysarthria, among other pathologies. This individual also had a de novo chromosome 5 duplication and a chromosome 2 duplication, while the 6p loss was implied benign, being inherited from his apparently unaffected father. Nevertheless, this rare description in Decipher and the precise location are striking.

A possible explanation for how a gain could influence nearby gene expression during palate development is via disruption of a local topologically associated domain (TAD; Lupiáñez et al. 2016; Thieme and Ludwig 2017). TADs—which define boundary regions where DNA sequences such as promoter-enhancer contacts occur—are often marked by CTCF binding sites. Although cells relevant to fetal uvula development have not yet been investigated, numerous CTCF binding sites conserved across multiple cell lines have been identified (http://genome.ucsc.edu/). These include at least one within the CNV immediately distal to *FOXF2*, which, by

impacting a relevant TAD, could compound with the effect of the missense mutation. In the context of the family reported here, given the proximity and shared segregation, it is therefore difficult to rule out a role for both the CNV and the missense variant in the causality of the uvula phenotype.

Mammals have 2 *FoxF* genes: *FoxF1* and *FoxF2* (previously *FREAC-1* and *FREAC-2* in humans; *FoxF2* was also known as *Lun* in mouse; Clevidence et al. 1994; Pierrou et al. 1994; Miura et al. 1998; Carlsson and Mahlapuu 2002). The expression pattern of *Foxf2* includes the mesenchyme of the oral cavity and the tongue, but it is also present in fetal and adult lung and the placenta, with low levels in the prostate, small intestine, colon, and fetal brain. It is, however, strongly expressed in the posterior secondary palate immediately prior to and during palatal shelf fusion, and $Foxf2^{-/-}$ mutants die at birth with a cleft of the secondary palate (Wang et al. 2003; Xu et al. 2016; Nik et al. 2016). *Foxf1* is more widely expressed in early embryogenesis, and knockout mice die by midgestation caused by vasculature abnormalities (Ormestad et al. 2004).

FOXF2 is well characterized as a transcription factor, consisting of a DNA binding domain and 2 transcriptional activation domains (AD1 and AD2; Blixt et al. 1998). *Foxf2* is a downstream target of an epithelia-mesenchymal interaction in the developing palate that involves FGF signaling in the mesenchyme, which in turn activates *Shh* expression in the epithelium (Nik et al. 2016; Xu et al. 2016). This pathway is also linked to TGFβ signaling, which explains consequential mesenchymal hypoplasia and cleft palate in mutants.

The p.Q433P variant in *FOXF2* is located within AD1 (Hellqvist et al. 1998) and was predicted to be damaging by bioinformatics analysis. We therefore investigated transcriptional activity of WT and p.Q433P FOXF2 proteins with a luciferase reporter assay in HeLa and HepG2 cells as previously described (Hellqvist et al. 1998). Surprisingly, we found that the variant resulted in significant upregulation of FOXF2 protein. Since transcript levels were constant, this might be explained by more efficient protein translation or by increased protein stability. Alternatively, high levels of overexpressed WT protein might be problematic for the cells; therefore, translation is actively restricted or the protein rapidly degraded. None of these possibilities were investigated further here but would be interesting to pursue in future work. In the context of increased protein levels, the reporter analysis showed a net increase in luciferase activity as compared with WT. However, expression levels are driven by the constitutive CMV promoter in the construct and thus is not designed to replicate regulation of this locus in vivo. By expressing the activity as a factor of the protein level, the variant resulted in a considerable loss of activity, which might more truly reflect the result of mutation in the activation domain. It was therefore interesting to note a comparative increase in *FGF18* expression in HeLa cells overexpressing mutant versus WT FOXF2, which was the same general trend observed for mice lacking *Foxf2* (Nik et al. 2016). Despite these cells not being a biologically relevant cell type for native *FOXF2* expression, overall a similar effect was replicated.

Further evidence for a role of *FOXF2* in orofacial clefts was reported by Bu et al. (2015), who identified an association between 2 intronic SNPs and their concordance with nonsyndromic cleft of the lip and/or the palate in an Asian population. As such, in an attempt to further investigate *FOXF2*, we chose to sequence a cohort of patients with cleft palate and SMCP. In the absence of other cases with an absent uvular phenotype, these patients were considered the most likely to be on the same phenotypic spectrum, especially since SMCP is often associated with bifid uvula. However, no likely causal mutations were identified. Instead, only 2 rare but "benign" missense variants from the N-terminal portion of the protein were detected. It is possible that patients with nonsyndromic cleft lip with or without cleft palate might have represented a better cohort, as suggested by the association data (Bu et al. 2015), but this remains to be tested. Furthermore, noncoding regulatory elements should not be ignored (Seto-Salvia and Stanier 2014; Thieme and Ludwig 2017). Nevertheless, our data potentially reflect the rarity of the absent uvula phenotype and lack of phenotype-genotype overlap with other palate anomalies.

In conclusion, while *FOXF2* is strongly implicated for absent uvula, nearby chromosomal duplications are confounding factors that may also contribute, potentially in combination with the *FOXF2* variant, by affecting transcriptional regulation of this or nearby genes. Further detailed analysis will be required to investigate the precise mechanisms involved. It would therefore be helpful to identify further families with a similar phenotype who also have mutations in this gene or nearby CNVs to further dissect their individual roles.

Author Contributions

R. Seselgyte, contributed to conception, design, and data analysis, drafted and critically revised the manuscript; D. Bryant, C. Demetriou, M. Ishida, E. Peskett, N. Moreno, D. Morrogh, M. Lees, M. Farrall, contributed to data analysis, critically revised the manuscript; D. Sell, contributed to conception, design, and data analysis, critically revised the manuscript; G.E. Moore, B. Sommerlad, E. Pauws, contributed to conception and design, critically revised the manuscript; P. Stanier, contributed to conception and design, drafted and critically revised the manuscript. All authors gave final approval and agree to be accountable for all aspects of the work.

Acknowledgments

We thank the Egyptian family for providing biological samples and clinical information. We are also grateful to Peter Carlsson for discussion and advice regarding the transient transfection experiments. A studentship to R.S. and the project was funded by CLEFT–Bridging the Gap. The human embryonic and fetal material was provided by the Joint MRC/Wellcome Trust (grant 099175/Z/12/Z) Human Developmental Biology Resource, and we thank Dianne Gerrelli for assistance with the in situ hybridization studies. P.S. is supported by the Great Ormond Street Hospital Children's Charity. This research was also supported by the Great Ormond Street Hospital Biomedical Research Centre, National

Institute for Health Research. The views expressed are those of the authors and not necessarily those of the National Health Service, the National Institute for Health Research, or the Department of Health. The authors declare no potential conflicts of interest with respect to the authorship and/or publication of this article.

ORCID iD

P. Stanier https://orcid.org/0000-0001-9340-8117

References

Aldinger KA, Lehmann OJ, Hudgins L, Chizhikov VV, Bassuk AG, Ades LC, Krantz ID, Dobyns WB, Millen KJ. 2009. FOXC1 is required for normal cerebellar development and is a major contributor to chromosome 6p25.3 Dandy-Walker malformation. Nat Genet. 41(9):1037–1042.

Blixt A, Mahlapuu M, Bjursell C, Darnfors C, Johannesson T, Enerback S, Carlsson P. 1998. The two-exon gene of the human forkhead transcription factor FREAC-2 (FKHL6) is located at 6p25.3. Genomics. 53(3):387–390.

Bu L, Chen Q, Wang H, Zhang T, Hetmanski JB, Schwender H, Parker M, Chou YH, Yeow V, Chong SS, et al. 2015. Novel evidence of association with nonsyndromic cleft lip with or without cleft palate was shown for single nucleotide polymorphisms in FOXF2 gene in an asian population. Birth Defects Res A Clin Mol Teratol. 103(10):857–862.

Calnan J. 1954. Submucous cleft palate. Br J Plast Surg. 69(4):264–282.

Carlsson P, Mahlapuu M. 2002. Forkhead transcription factors: key players in development and metabolism. Dev Biol. 250(1):1–23.

Clevidence DE, Overdier DG, Peterson RS, Porcella A, Ye H, Paulson KE, Costa RH. 1994. Members of the HNF-3/forkhead family of transcription factors exhibit distinct cellular expression patterns in lung and regulate the surfactant protein B promoter. Dev Biol. 166(1):195–209.

de Blacam C, Smith S, Orr D. 2018. Surgery for velopharyngeal dysfunction: a systematic review of interventions and outcomes. Cleft Palate Craniofac J. 55(3):405–422.

Firth HV, Richards SM, Bevan AP, Clayton S, Corpas M, Rajan D, Van Vooren S, Moreau Y, Pettett RM, Carter NP. 2009. Decipher: database of chromosomal imbalance and phenotype in humans using Ensembl resources. Am J Hum Genet. 84(4):524–533.

Gould DB, Mears AJ, Pearce WG, Walter MA. 1997. Autosomal dominant Axenfeld-Rieger anomaly maps to 6p25. Am J Hum Genet. 61(3):765–768.

Harville EW, Wilcox AJ, Lie RT, Vindenes H, Abyholm F. 2005. Cleft lip and palate versus cleft lip only: are they distinct defects? Am J Epidemiol. 162(5):448–453.

Hellqvist M, Mahlapuu M, Blixt A, Enerback S, Carlsson P. 1998. The human forkhead protein FREAC-2 contains two functionally redundant activation domains and interacts with TBP and TFIB. J Biol Chem. 273(36):23335–23343.

Kaplan EN. 1975. The occult submucous cleft palate. Cleft palate J. 12(1):356–368.

Lehmann OJ, Ebenezer ND, Jordan T, Fox M, Ocaka L, Payne A, Leroy BP, Clark BJ, Hitchings RA, Povey S, et al. 2000. Chromosomal duplication involving the forkhead transcription factor gene FOXC1 causes iris hypoplasia and glaucoma. Am J Hum Genet. 67(5):1129–1135.

Lupiáñez DG, Spielmann M, Mundlos S. 2016. Breaking TADs: how alterations of chromatin domains result in disease. Trends Genet. 32(4):225–237.

Mardini S, Chim H, Seselgyte R, Chen PK. 2016. Predictors of success in furlow palatoplasty for submucous clefts: an experience with 91 consecutive patients. Plast Reconstr Surg. 137(1):135e–141e.

Meskin LH, Gorlin RJ, Isaacson RJ. 1964. Abnormal morphology of the soft palate: I. The prevalence of cleft uvula. Cleft Palate J. 35(1):342–346.

Miura N, Kakinuma H, Sato M, Aiba N, Terada K, Sugiyama T. 1998. Mouse forkhead (winged helix) gene Lun encodes a transactivator that acts in the lung. Genomics. 50(3):346–356.

Mossey PA, Little J, Munger RG, Dixon MJ, Shaw WC. 2009. Cleft lip and palate. Lancet. 374(9703):1773–1785.

Nik AM, Johansson JA, Ghiami M, Reyahi A, Carlsson P. 2016. Foxf2 is required for secondary palate development and Tgfbeta signaling in palatal shelf mesenchyme. Dev Biol. 415(1):14–23.

Ormestad M, Astorga J, Carlsson P. 2004. Differences in the embryonic expression patterns of mouse Foxf1 and -2 match their distinct mutant phenotypes. Dev Dyn. 229(2):328–333.

Pauws E, Hoshino A, Bentley L, Prajapati S, Keller C, Hammond P, Martinez-Barbera JP, Moore GE, Stanier P. 2009. Tbx22null mice have a submucous cleft palate due to reduced palatal bone formation and also display ankyloglossia and choanal atresia phenotypes. Hum Mol Genet. 19(15):4171–4179.

Perry JL. 2011. Anatomy and physiology of the velopharyngeal mechanism. Semin Speech Lang. 32(2):83–92.

Pierrou S, Hellqvist M, Samuelsson L, Enerback S, Carlsson P. 1994. Cloning and characterization of seven human forkhead proteins: binding site specificity and dna bending. EMBO J. 13(20):5002–5012.

Sell D, Harding A, Grunwell P. 1999. Gos.Sp.Ass.'98: an assessment for speech disorders associated with cleft palate and/or velopharyngeal dysfunction (revised). Int J Lang Commun Disord. 34(1):17–33.

Seto-Salvia N, Stanier P. 2014. Genetics of cleft lip and/or cleft palate: association with other common anomalies. Eur J Med Genet. 57(8):381–393.

Sommerlad BC, Fenn C, Harland K, Sell D, Birch MJ, Dave R, Lees M, Barnett A. 2004. Submucous cleft palate: a grading system and review of 40 consecutive submucous cleft palate repairs. Cleft Palate Craniofac J. 41(2):114–123.

Stanier P, Moore GE. 2004. Genetics of cleft lip and palate: syndromic genes contribute to the incidence of non-syndromic clefts. Hum Mol Genet. 13 Spec No. 1:R73–R81.

Swanson JW, Mitchell BT, Cohen M, Solot C, Jackson O, Low D, Bartlett SP, Taylor JA. 2017. The effect of furlow palatoplasty timing on speech outcomes in submucous cleft palate. Ann Plast Surg. 79(2):156–161.

Thieme F, Ludwig KU. 2017. The role of noncoding genetic variation in isolated orofacial clefts. J Dent Res. 96(11):1238–1247.

Wang T, Tamakoshi T, Uezato T, Shu F, Kanzaki-Kato N, Fu Y, Koseki H, Yoshida N, Sugiyama T, Miura N. 2003. Forkhead transcription factor Foxf2 (Lun)-deficient mice exhibit abnormal development of secondary palate. Dev Biol. 259(1):83–94.

Xu J, Liu H, Lan Y, Aronow BJ, Kalinichenko VV, Jiang R. 2016. A Shh-Foxf-Fgf18-Shh molecular circuit regulating palate development PLOS Genet. 12(1):e1005769.